Journal of Chromatography A, 1218 (2011) 2984–2994

Contents lists available at ScienceDirect

Journal of Chromatography A

journal homepage: www.elsevier.com/locate/chroma

An experimental study of sampling time effects on the resolving power of on-line two-dimensional high performance liquid chromatography

Yuan Huang[a], Haiwei Gu[a], Marcelo Filgueira[a,b], Peter W. Carr[a,*]

[a] Department of Chemistry, Smith and Kolthoff Halls, University of Minnesota, 207 Pleasant St. S.E., Minneapolis, MN 55455, USA
[b] Univ Nacl La Plata, Div Quim Analit, Fac Ciencias Exactas, RA-1900 La Plata, Argentina

ARTICLE INFO

Article history:
Received 2 October 2010
Received in revised form 21 February 2011
Accepted 16 March 2011
Available online 12 April 2011

Keywords:
Two dimensional liquid chromatography
Sampling time
Optimization
Peak capacity
Resolving power

ABSTRACT

The experimental effects of sampling time on the resolving power of on-line LC × LC were investigated. The first dimension gradient time (^1t_g) and sampling time (t_s) were systematically varied (^1t_g = 5, 12, 24 and 49 min; t_s = 6, 12, 21 and 40 s). The resolving power of on-line LC × LC was evaluated in terms of two metrics namely the numbers of observed peaks and the effective 2D peak capacities obtained in separations of extracts of maize seeds. The maximum effective peak capacity and number of observed peaks of LC × LC were achieved at sampling times between 12 and 21 s, at all first dimension gradient times. In addition, both metrics showed that the "crossover" time at which fully optimized 1DLC and LC × LC have equal resolving power varied somewhat with sampling time but is only about 5 min for sampling times of 12 and 21 s. The longest crossover time was obtained when the sampling time was 6 s. Furthermore, increasing the first dimension gradient time gave large improvements in the resolving power of LC × LC relative to 1DLC. Finally, comparisons of the corrected and effective 2D peak capacities as well as the number of peaks observed showed that the impact of the coverage factor is quite significant.

1. Introduction

Due to its much higher resolving power as compared to one dimensional liquid chromatography [1–10], comprehensive two dimensional liquid chromatography is now receiving increased attention for the separation of complex samples. Complex samples such as typical proteomic [11] and metabolomic [12] samples can contain thousands of constituents covering a very wide range of concentrations. One dimensional column liquid chromatography is often not able to provide sufficient resolving power for the analysis of such samples [5,13,14]. As a result, comprehensive two-dimensional LC (subsequently here denoted as LC × LC [15]) has been used for complex samples in the fields of proteomics [11,16–18], metabolomics [3,4,19,20], synthetic polymers [21–23] and oil and fat analysis [24].

There are two primary variants of LC × LC [1–10,25–27]. In off-line LC × LC [7,8,26,27], fractions from the first dimension column effluent are first collected, stored and then re-injected into a second dimension column. In this mode, the first and second dimension separations are essentially independent processes. In on-line LC × LC, the first and second dimension separations are carried out concurrently [1,3–7,9,10,26,27]. The on-line variant of LC × LC mandates that the second dimension separation be completed during the time that the effluent fraction from the first dimension is collected; this is frequently done on the sub-minute time scale [3–6]. It should be pointed out that even for fast second dimension analysis, peak broadening resulting from excessive under-sampling of the first-dimension peaks still causes a substantial decrease in the overall resolving power of on-line LC × LC [28–31]. In other words, when the first dimension separation is sampled and transferred, some of the first dimension resolution is lost. In addition, due to limitations on the volume of the fractions that can be transferred to the second dimension column, the first dimension separation of on-line LC × LC is usually operated under sub-optimum conditions [4–6]; this causes further losses in the effective peak capacity compared to fully optimized 1DLC. The loss in the first dimension peak capacity is traded-off for gains in the peak capacity of the second dimension separation. It is obvious that when the peak capacity gained in the second dimension does not at least compensate for the lost of first dimension peak capacity converting a 1DLC separation to a LC × LC separation will not improve the resolving power, and the 1D method should be preferred. The determination of which methodology will have the better resolving power is analytically very important and relevant to the question of which method is the more appropriate for a specific application. Unfortunately, only a few papers have systematically compared the separation performance of 1DLC and LC × LC [3,32].

* Corresponding author. Tel.: +1 612 624 0253; fax: +1 612 626 7541.
E-mail addresses: carr@chem.umn.edu, petecarr@umn.edu (P.W. Carr).

0021-9673/$ – see front matter © 2011 Elsevier B.V. All rights reserved.
doi:10.1016/j.chroma.2011.03.032

A detailed experimental comparison of the resolving power of on-line LC × LC and fully optimized 1DLC was carried out by Stoll et al. [3]. In that work, the resolving power of fully optimized 1DLC and the best achievable on-line LC × LC were compared. According to Stoll's results [3], with increasing analysis time, on-line LC × LC will eventual surpass 1DLC. In addition, by extrapolating their results they estimated that the crossover time at which both 1DLC and on-line LC × LC give comparable resolving power takes place in 5–10 min for the conditions used in their work based on the behavior of a maize extract. However, their work was done at only one sampling time (21 s) and to find the crossover time they had to extrapolate. Based on the theoretical calculations of Li [1], Horvath [7], and Potts [33], we know that sampling time should have a very large impact on the overall resolving power of on-line LC × LC.

The primary objective of the present work was to experimentally examine the effect of sampling time on the comparison of 1DLC and on-line LC × LC and compare the results to theory. The principal question is: does the resolving power of LC × LC show an optimum at intermediate values of the sampling time? Subsidiary issues include whether the first dimension gradient time impacts the position of the optimum and is the crossover time truly in the range of 5–10 min or does it vary with sampling time. A major experimental goal of this work was to measure the resolving power of LC × LC as a function of the first dimension gradient time and sampling time using the separation of a real sample; this has not yet been reported.

2. Theory

A fair comparison of 1DLC and on-line LC × LC requires that both of these methods be performed so that each gives the best possible separation performance. Therefore, in order to consider this comparison, we need to consider the theory of optimization in 1DLC and on-line LC × LC.

For conventional 1DLC optimization, Wang et al. developed and validated a computational approach to gradient elution RPLC that allows the full optimization of peak capacity in a given gradient time through the accurate prediction of peak widths and retention times for the compounds of interest [34–36] as a function of column length, linear velocity, and gradient composition, at a fixed column diameter and particle size while operating at the maximum operating pressure and column temperature. This approach was generally followed in this work. In contrast to 1DLC, optimization of on-line LC × LC is much more complicated since additional limitations [3] have to be imposed on the operational parameters, such as the first dimension flow rate [3] and sampling time [1,29]. For the first dimension separation, there is a severe constraint on the volume of first dimension effluent that can be delivered to the second dimension column. Because injection of an overly large volume of effluent from the first dimension will cause serious peak broadening in the second dimension separation, the first dimension separation generally has to be carried out at sub-optimum flow rates, which greatly restricts the range of the flow rates that can be considered for optimization.

In comparing the peak capacity of 1D-LC and LC × LC Stoll et al. used the following conventional definition of the 1D peak capacity [3]:

$$n_{c,1D} = \frac{t_{R,last} - t_{R,first}}{w_{avg.}} \quad (1)$$

where $t_{R,\,last}$ and $t_{R,\,first}$ are the retention times of the last and first peaks observed in the separation space and $w_{avg.}$ is the average 4σ peak width. This is the quantity optimized in the method of Wang [34–36]. However, in the case of on-line LC × LC Stoll [3] defined an effective peak capacity as follows:

$$n^{*}_{c,2D} = {}^{1}n_c \times {}^{2}n_c \times f_{coverage} \times \frac{1}{\langle\beta\rangle} \quad (2)$$

This was done to correct the so-called product rule for two problems. The first corrects for under-sampling of the first dimension [28,29] through use of the Davis–Stoll–Carr correction factor [3], $(1/\langle\beta\rangle)$ here re-written in the form derived by Li [1] and by Potts [33] and used in alternative forms by Guiochon [7,8] and by Schoenmakers [37]:

$$\langle\beta\rangle = \sqrt{1 + 3.35\left(\frac{{}^{2}t_c}{{}^{1}w}\right)^{2}} \quad (3)$$

In this equation ${}^{2}t_c$, is the second dimension gradient cycle time which in on-line LC × LC is equal to the sampling time (t_s), The second correction factor is $f_{coverage}$. This is an approximate correction for the fact that the whole separation space is never used. Stoll used a modification of a method developed by Gilar [3,32]. In her work Li approximated the numerator in Eq. (1) as ${}^{1}t_g$ the first dimension gradient time and then by examining the limit of on-line LC × LC peak capacity under conditions of severe under-sampling she found that the corrected peak capacity (assuming $f_{coverage}$ was 1.0) could be approximated as [1]:

$$n'_{c,2D} = \frac{{}^{1}t_g\,{}^{2}n_c}{1.83\,{}^{2}t_c} \quad (4)$$

Eq. (4) will be referred to repeatedly in this work.

Several papers have appeared on the optimization of comprehensive on-line LC × LC systems [1,7,28,33,37,38]. Schoenmakers et al. suggested a protocol for its optimization based on the concept of Poppe plots [38]. However, instead of optimizing the sampling time, this protocol simply took the sampling time as being equal to the first dimension standard deviation (${}^{1}\sigma$). This is known to be much too fast [29,31]. Thus no correction is made for the first dimension under-sampling effect discussed above [1,29,31] as it is assumed to be unimportant at such a fast sampling rate. Since the sampling time is a very important parameter for the optimization of the overall resolving power of LC × LC [1,7,33,39], operational conditions obtained from this protocol were evidently not fully optimized. Subsequently Horie et al. using Seeley's model of the under-sampling correction studied the optimum value of the sampling time [28,30]. More recently the Schoenmaker's group published a comprehensive paper on on-line LC × LC optimization, which took into consideration both the under-sampling effect and peak broadening caused by large injection volumes in the second dimension. Particle sizes, column diameters, column lengths and the velocity of both dimensions as well as optimum sampling time were optimized simultaneously. The effects of using isocratic and gradient elution and their various combinations in both dimensions were studied. Conventional HPLC and UPLC systems and their combinations in both dimensions were studied using gradient elution in both dimensions. A Pareto-optimality method was used to find the best compromise between the different objectives including the maximum peak capacity, the minimum analysis time and sample dilution [37].

Eq. (4) provides a useful and straightforward guide for on-line LC × LC optimization. First, this equation shows that the second dimension peak capacity production rate (${}^{2}n_c/{}^{2}t_c$) is critical to the optimization of 2D peak capacity [33]. Second, according to this equation, the first dimension peak capacity is not critical to the overall peak capacity [1]; this was later confirmed [7,33]. Since the first dimension peak capacity is not as critical to the overall 2D separation power as is that of the second dimension [1,7,33], the sub-optimal first dimension peak capacities resulting from the

inability to optimize the flow rate of the first dimension are not critical to the overall 2D peak capacity. Furthermore, this equation shows that the first dimension gradient time plays an important role in the overall resolving power of on-line LC × LC.

3. Experimental

3.1. Chemicals

The standards used to determine peak capacities (tyrosine, 5-hydroxy-L-tryptophan, tryptophan, indole-3-acetic acid, indole-3-propionic acid, and indole-3-acetonitrile) were purchased from Sigma–Aldrich (St. Louis, MO) as reagent grade or better. Acetonitrile was obtained from Burdick and Jackson (Muskegon, MI). Sodium dihydrogen phosphate was from JT Baker (Phillipsburg, NJ), and sodium monohydrogen phosphate was obtained from Fisher Scientific (Fairlawn, NJ). HPLC grade water was from Sigma–Aldrich (St. Louis, MO). All materials were used as received.

All aqueous eluents were prepared gravimetrically (±0.01 g) and passed through 0.45 μm nylon membrane filtration apparatus (Lida Manufacturing Inc., Kenosha, WI) immediately before use.

3.2. Sample preparation

The standard solutions used to assess the accuracy of peak capacity predictions contained sodium nitrate, tyrosine, 5-hydroxy-L-tryptophan, tryptophan, indole-3-acetic acid, indole-3-propionic acid, and indole-3-acetonitrile. These compounds were dissolved in 20 mM sodium phosphate buffer, pH 5.7 at concentrations of 20 μg/mL. The corn seed used for 1DLC and on-line LC × LC separations was Silver Queen (Burpee, Warminster, PA) and was extracted as follows: 40 g of whole seed were ground to a fine, dry powder using a blender. The powder was then divided into eight approximately equal aliquots. Each portion was then transferred to a 20 mL glass vial, followed by addition of 3.5 mL of methanol and 1.5 mL 20 mM phosphate buffer (pH 5.7). Each resulting mixture was sonicated in an ultrasonic bath (model PC3, L&R Manufacturing, Kearny, NJ) at room temperature for 2 h, followed by centrifugation at 3000 rpm for 15 min. The eight resulting supernatant solutions were then collected together into a 32 mL glass vial, resulting in a solution of about 8 mL. 20 mL of 20 mM sodium phosphate buffer (pH 5.7) were then added to the resulting solution under mild stirring to precipitate the highly hydrophobic components. The mixture was then centrifuged for 20 min at 3000 rpm to pellet the remaining insoluble material. The resulting supernatant was then filtered through a 0.45 μm filter, resulting in 18 mL of clear solution. This solution, which will be called solution A in the following procedure, was then concentrated using C_{18} and carbon SPE cartridges as follows.

A C_{18} SPE cartridge (500 mg, Agilent Technologies; Wilmington, DE) was first conditioned by passing 3 mL of methanol and then 3 mL of 90:10 deionized water–methanol through it. After conditioning, all 18 mL of solution A was loaded onto the SPE cartridge. The filtrate (solution B) from the cartridge was collected during this process. After solution A passed completely through the cartridge 1 mL of 50:50 20 mM phosphate buffer (pH 5.7)–acetonitrile solution was passed through the cartridge to recover the retained components. The recovered solution is called solution C.

A carbon cartridge (500 mg, SimpleQ, from Agilent) was first conditioned in the same way as the C_{18} SPE cartridge. Then solution B was loaded on the carbon cartridge. This cartridge was then flushed with 3 mL of tetrahydrofuran (THF). The THF recovered from this cartridge was collected in a 20 mL glass vial and then evaporated under gentle nitrogen flow, resulting in a light yellow precipitate at the bottom of the vial. Finally, solution C was transferred to this vial followed by sonication for about 10 min until the light yellow precipitate at the bottom completely dissolved. The resulting sample of approximately 1 mL was stored in a freezer and analyzed without further treatment.

Table 1
Operational parameters and peak capacities for fully optimized one dimensional liquid chromatography.

t_g (min)[a]	5	12	24	52
L (cm)[b]	20	30	40	50
F (mL/min)[c]	1.1	0.65	0.45	0.35
ϕ_i [d]	0	0	0	0
ϕ_f [e]	0.7	0.6	0.5	0.38
$n_{c,\,measured}$ [f]	100	135	150	163
$n_{c,\,pred}$ [g]	111	137	151	162

[a] Gradient time.
[b] Column length.
[c] Flow rate. All columns are 2.1 mm in diameter.
[d] Initial eluent strength.
[e] Final eluent strength.
[f] Peak capacity calculated by Eq. (1) using the average peak width of standards measured experimentally under the operational conditions listed in this table.
[g] Peak capacity predicted by the optimization procedure reported in Ref. [3]. Operation temperature was 40 °C. Maximum system pressure was 400 bar. Solvent A: 20 mM phosphate buffer at pH = 5.7. Solvent B: acetonitrile.

3.3. Instrumentation

3.3.1. 1DLC instrument

Conventional 1D separations were performed using an Agilent 1100 liquid chromatograph controlled by version B.01.03 Chemstation software (Agilent Technologies; Wilmington, DE). This instrument was equipped with an Agilent 1100 capillary pump (Model Number G1376A), an autosampler (Model Number G1329A), column thermostating compartment (Model Number G1316B) and a variable wavelength UV detector (Model Number G1314A). The detector wavelength was set at 220 nm. Reversed phase separations were carried out with various Discovery HS-F5 columns (Supelco, Bellefonte, PA, 2.1 mm i.d., 5 μm particle diameter) using gradient elution. The A solvent was a 20 mM aqueous phosphate buffer at pH 5.7. The B solvent was pure acetonitrile. Operational parameters, including column length, flow rate, and mobile phase compositions at given gradient times were optimized simultaneously using the Solver function of Microsoft Excel [3,36], with the following constraints. The maximum allowable system pressure was set to 400 bar. The initial mobile phase composition was fixed at 100% aqueous buffer. The maximum column length was set to 50 cm, and the column inner diameter was fixed at 2.1 mm. The flow rate was allowed to vary between 0.1 and 5 mL/min. The final composition of eluent was allowed to vary from 10 to 100% organic modifier (v/v). The "optimum" operational conditions were achieved when the peak capacity was maximized at the desired gradient time. The operational parameters, peak capacities predicted by the previously reported procedure [3] and peak capacities measured experimentally in this study are listed in Table 1. For all the fully optimized 1DLC experiments in this study, the operational conditions are listed in Table 1 unless otherwise noted in the text. The effective gradient delay volume of this system was measured to be 1.0 mL, using the conventional technique [40]. Delayed injection was used for all gradient elution runs.

3.3.2. 2D instrument-first dimension

The basic configuration of the on-line LC × LC system used in this work was described in a previous publication [3] (see Fig. 1). The first dimension of the on-line LC × LC system used an Agilent 1100 quaternary pump (G1311A). All the other components are the same as the 1D separations described above, including the solvents, columns and other instrumental components. The

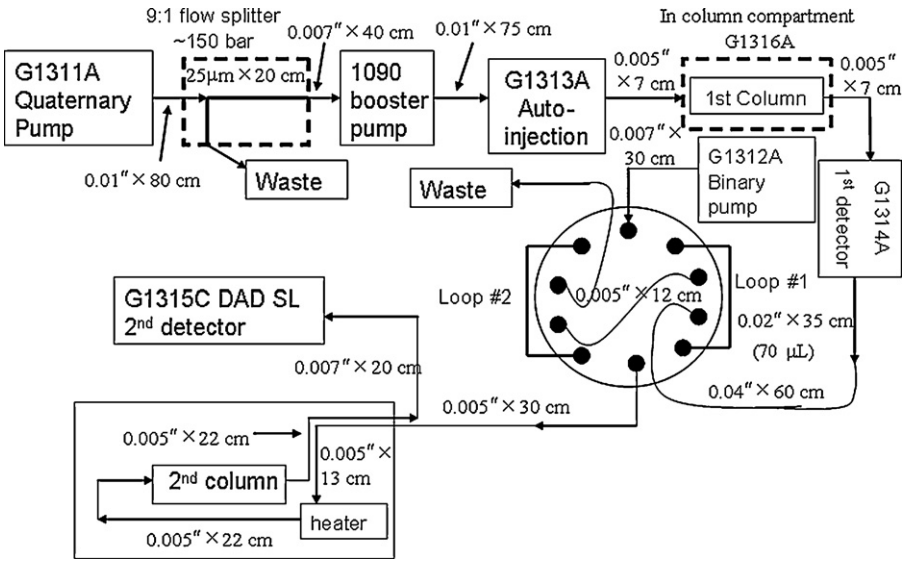

Fig. 1. Complete configuration of instrument used for fast on-line two dimensional liquid chromatography separation. Sizes of all connecting tubes are given in diagram.

only difference from the 1D separation is that the flow rate of the first dimension of LC × LC was fixed at 0.10 mL/min; this was obtained using a 9:1 flow-splitter as reported previously [3]. The outlet of the first-dimension detector was connected to a 10-port valve (VICI CHEMINERT 09v-0233H, Valco Instruments, Houston, TX) shown in Fig. 1. The 10-port valve was actuated pneumatically using helium at 50 psi. The two sample loops (loop 1 and loop 2 in Fig. 1) were made of 35 cm long 0.02-in.-i.d. PEEK tubing; the volume of each loop was 70 μL in all experiments. As shown in Fig. 1, the 10-port valve was plumbed in a "first in-last out" (FILO) manner. Optimization of the first dimension was done by varying the column length and gradient composition while fixing the flow rate at 100 μL/min, as has been shown in prior work from this lab [3,36,39]. In this study, all the experiments were performed using FILO valve configuration unless otherwise noted in the text. The operational conditions and measured peak capacities of the first dimension separation in on-line LC × LC are given in Table 2.

3.3.3. 2D instrument-second dimension

An Agilent 1100 binary pump (Model Number G1312A) was used in the second dimension of the on-line LC × LC system. The operational parameters for the second dimension separations are listed in Table 2. The A solvent was the 10 mM aqueous phosphoric acid buffer described above. The B solvent was pure acetonitrile. The second dimension gradient time was variously set as 3, 9, 18 and 37 s, with a fixed re-equilibration time of 3 s regardless of the gradient time. The data sampling rate of the detector was 80 Hz with the DAD detector (Agilent Model G1315C SL). All data in this paper are at 220 nm. The components of the whole on-line LC × LC system, including the first dimension pump, autosampler, 10-port valve, second dimension pump and detector were coordinated by LabVIEW 7.0 software via a 6024E data acquisition board (National Instruments Inc., Austin, TX) using a program written in-house [3].

The second dimension separation was carried out on 2.1 mm × 33 mm columns packed with 3.0 μm diameter carbon-clad zirconia reversed-phase material (8%, w/w, carbon, ZirChrom Separations, Inc.; Anoka, MN). The column was operated at 110 °C at a flow rate of 3.0 mL/min, corresponding to a maximum system pressure of ~340 bar during gradient elution. An eluent pre-heater and column heating jacket from Systec Inc. (New Brighton, MN) were used to pre-heat and maintain the mobile phase to the second dimension column at 110 ± 0.1 °C. Columns with the small inner diameter were used to minimize the thermal mismatch peak broadening caused by the radial temperature gradient in the column [41]. In addition, the small dimensions of this column

Table 2
Operational parameters used for on-line two dimensional liquid chromatography separations, and experimental first dimension peak capacities.

	First dimension					Second dimension			
^1t_g [a] (min)	5	12	24	49	^2t_g [g] (s)	3	9	18	37
L (cm)[b]	5	10	10	20	L (cm)[h]	3.3	3.3	3.3	3.3
F (mL/min)	0.1	0.1	0.1	0.1	F (mL/min)	3.0	3.0	3.0	3.0
ϕ_i [c]	0	0	0	0	ϕ_i [i]	0	0	0	0
ϕ_f [d]	0.65	0.6	0.5	0.45	ϕ_f [j]	1.0	1.0	1.0	0.7
^1w (min)[e]	0.183	0.207	0.310	0.524					
^1n_c [f]	27	58	78	94					

For the second dimension separation, solvent A was 10 mM phosphoric acid. Solvent B was acetonitrile. Temperature, 110 °C. Column, 2.1 mm i.d. ZirChrom-CARB (8% carbon, w/w).

[a] First dimension gradient time.
[b] Column length of the first dimension.
[c] Initial eluent strength in first dimension.
[d] Final eluent strength in first dimension.
[e] Average 4σ first dimension peak width based on the experimental measurement of the indole standards under the operational conditions listed in this table.
[f] First dimension peak capacity calculated by Eq. (1).
[g] Second dimension gradient time. $t_s = {}^2t_g + 3$ s. 3 s is the re-equilibration time.
[h] Column length in second dimension.
[i] Initial eluent strength in the second dimension. For the first dimension separation, solvent A was 20 mM phosphate buffer at pH = 5.7.
[j] Final eluent strength in the second dimension. Solvent B was acetonitrile. Temperature, 40 °C. Column, 2.1 mm i.d. Discovery HS-F5.

also allow us to have a good detection sensitivity on the second dimension. Finally, the small dimensions of this column together with the high flow rate ensure a short system dwell time and fast column re-equilibration [42,43]. Carbon-clad zirconia was chosen as the second dimension phase for its good chemical and mechanical stability at high temperature, high flow rate conditions, and most importantly its high degree of orthogonal selectivity relative to other RPC phases [4]. Also the carbon phase is rather retentive relative to the HS-F5 first dimension phase [4]. The strong retentivity of the carbon stationary phase is essential to focusing the first dimension effluents at the inlet of the second dimension column while still allowing us to use small column dimensions. Such a focusing process is critical to reducing the extra peak broadening caused by the large volume of the first dimension effluents injected into the second dimension column from the sample loops of the 10-port valve [4]. Gradient elution was used for the second dimension separation for several reasons: first, it greatly increases the second dimension peak capacity, which is critical to the overall resolving power of the LC × LC system. Second, it enables us to effectively focus the first dimension effluent at the inlet of the carbon stationary phase [4]. The initial mobile phase was fixed at 100% aqueous buffer. The final mobile phase composition that leads to the distribution of sample components over the entire gradient time window at a given gradient time was chosen. Operational conditions of both dimensions of all the on-line LC × LC experiments are given in Table 2, unless otherwise noted in the text.

3.4. Calculation of 1DLC and on-line LC × LC peak capacities

The peak capacity of the fully optimized 1D gradient elution separations was estimated according to Eq. (1) [3]. For all 1D runs, since a delayed inject was used and the first peak in the maize seed extract was always observed eluting at the column dead time plus the system delay time, $t_{R,\,first}$ in Eq. (1) was taken as $t_m + t_d$. In addition, the operational conditions were optimized such that the last peak (indole-3-acetonitrile) in our standard sample eluted near the end of the gradient, $t_{R,\,last}$ was set equal to $t_m + t_d + t_g$. The peak width in Eq. (1) was taken as the average 4σ peak width of the six compounds in the standard mixture.

The effective 2D peak capacity of on-line LC × LC with a specific first and second dimension gradient time combination was calculated according to Eqs. (2) and (3). In our experiment, ${}^1n_c$ in Eq. (2) was measured by the same procedures as was the fully optimized 1DLC. The standard mixture was injected on the first dimension columns and separated under the relevant first dimension gradient elution operational conditions. The average peak width of these standard compounds was calculated. Values of $t_{R,\,first}$ and $t_{R,\,last}$ were taken as $t_m + t_d$ and $t_m + t_d + t_g$, respectively. The second dimension peak capacity ${}^2n_c$ was calculated based on the average of the observed 4σ peak widths of 10–20 representative well formed second-dimension peaks in the on-line LC × LC separations of the maize seed extract sample performed under the corresponding first and second dimension gradient times, and other operational conditions. These second dimension peaks were carefully chosen to avoid broad peaks caused by sample overloading, specific chemical interactions between the column and samples, and unresolved peaks. The value of ${}^2n_c$ was then calculated by the ratio of the second dimension gradient time, which is t_s – 3 s to the average 4σ peak width of the second dimension separation. After obtaining ${}^1n_c$ and ${}^2n_c$, the value of $\langle\beta\rangle$ for the effective 2D peak capacity calculation was obtained from Eq. (3) based on both the t_s value and the first dimension average peak width obtained in the ${}^1n_c$ calculation.

The value of $f_{coverage}$ was measured from the fraction of the separation space occupied by the maize seed extract sample peaks under the corresponding first and second dimension operational conditions. The details of coverage factor estimation were described previously [3] and are shown in Fig. S1. Generally, a grid was first drawn on the 2D chromatogram and the boundaries of the region occupied by real peaks of the maize seed extract sample were defined on the grid. The fraction of the bins in this region was then computed. For on-line LC × LC runs with first dimension gradient times of 5, 12 and 24 min, the size of the bins on the first dimension was taken as 1 min. For a gradient time of 49 min, 2 min was used as the first dimension bin size. It should be understood that $f_{coverage}$ is very dependent on the grid size used. For sampling times of 6, 12, 21 and 40 s the second dimension bin widths were taken as 0.5, 1, 2 and 4 s, respectively. The $f_{coverage}$ value was calculated by the ratio of the number of bins in the occupied region to the total number of bins in the grid.

3.5. Peak counting of the corn seed extract

The number of peaks in the separation of the maize seed extract was determined by visual inspection of the 2D chromatograms. The following criteria were followed for the visual inspection. The first is unimodality [44]. According to this criterion, among a set of peaks with the same second dimension retention time distributed in consecutive second dimension cycles, once a maximum intensity peak has been identified, then a peak in a subsequent cycle which is larger in magnitude than the earlier peak constitutes a new species and is counted as a new peak. Second, once a new potential maximum is visually identified, it has to be the local maximum among the neighboring 8 data points in the surrounding two-dimensional array. Such a local maximum test was performed by a Matlab program [3]. Third, when the 10-port sampling valve was connected in the so-called "first in-last out" (FILO) configuration, systematic variations in the second dimension retention times were observed (see Fig. S2). Such systematic variations were not observed when the 10-port sampling valve was connected in the "first in-first out" (FIFO) configuration. Fortunately, due to the alternate characteristics of the retention shift, identifying such a peak shift pattern by visual inspection is possible. Our peak counting results based on the same sample showed that under the same first and second dimension operational conditions, the differences in peak numbers counted with FILO and FIFO configurations were acceptably close and did not alter our conclusions.

4. Results and discussion

4.1. Effects of sampling time and first dimension gradient time on corrected 2D peak capacity

Fig. 2 shows the *corrected* 2D peak capacity versus the sampling time. The 2D peak capacities in Fig. 2 were corrected for the undersampling effect by using Eqs. (2) and (3), but the $f_{coverage}$ value was set to unity. The measured values of ${}^1n_c$ and the related first dimension peak widths that are required for the calculations are listed in Table 2. The second dimension peak capacities (${}^2n_c$) at different sampling times (t_s) were computed from Eq. (5):

$$ {}^2n_c = {}^2n_{c,\,limit} \times (1 - \exp(-\lambda \times {}^2t_g)) \quad (5) $$

where ${}^2n_c$ is the second dimension peak capacity and ${}^2n_{c,\,limit}$ is the limiting second dimension peak capacity that can be achieved at long gradient times for a column with a fixed length; ${}^2t_g$ is the second dimension gradient time (${}^2t_g = t_s - 3$ s) and λ defines how fast ${}^2n_c$ reaches its limiting value [33]. The values of ${}^2n_{c,\,limit}$ (=39.7) and λ (=0.11 s^{-1}) used in Eq. (5) were obtained by fitting the average experimental second dimension peak capacities as a function of sampling times (t_s = 6, 12, 21, 40 s). The peaks were acquired during real LC × LC separations of maize seed extracts at the four different

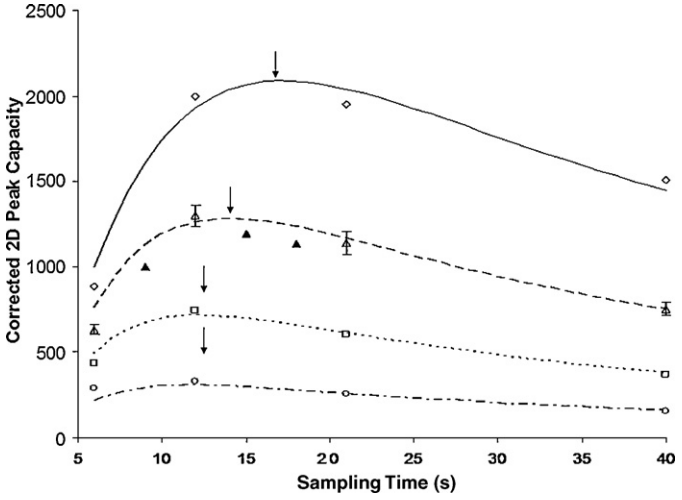

Fig. 2. Plot of corrected 2D peak capacity versus sampling time for on-line two dimensional liquid chromatography separation. The corrected 2D peak capacities are corrected for under-sampling effect using Eqs. (2) and (3), with $f_{coverage}$ set to unity. Curves are based on calculated corrected 2D peak capacities. Values of ${}^1n_c$ and first dimension peak width for the calculation are given in Table 2. ${}^2n_c$ values for the calculation were obtained using ${}^2n_c = 39.7 \times (1 - \exp(-0.11 \times {}^2t_g))$, where ${}^2t_g = t_s - 3$ s. This equation was obtained by fitting Eq. (5) using the average values of the second dimension peak capacities measured at 6, 12, 21, and 40 s sampling times. First dimension gradient times for the curves are 5 min (dashed and dotted line); 12 min (dotted line); 24 min (dashed line); 49 min (solid line). Arrows on curves indicate the maximum corrected 2D peak capacities. Symbols represent the corrected 2D peak capacities obtained from experimentally measured second dimension peak capacities. First dimension gradient times for symbols are 5 min (○); 12 min (□); 24 min (△) and (▲); 49 min (◊). (△) and error bars on the 24 min curve are the average and standard deviations of the corrected 2D peak capacities obtained from experimentally measured second dimension peak capacities based on 3 different on-line LC × LC separations of maize samples using 3 different second dimension columns. Two of these separations used the FIFO valve configuration. (▲) Symbols represent corrected 2D peak capacities obtained from experimentally measured second dimension peak capacities based on a single on-line LC × LC separation of maize sample using the FIFO configuration.

first dimension gradient times. The values of ${}^1n_c$, first dimension peak widths for different first dimension gradient times, and values of ${}^2n_c$ at different sampling times obtained were then used to calculate the corrected 2D peak capacities in Fig. 2 by use of Eqs. (2) and (3). An equation of the form of Eq. (5) was used here because our previous second dimension peak capacities measured based on both alkylphenone and peptide standards [1,33] were reasonably well fitted by this equation. However, the mathematical format of this equation has no fundamental significance [1].

Fig. 2 clearly shows that the maximum corrected 2D peak capacity was always obtained at an intermediate value of the sampling time. The existence of such an optimum sampling time is consistent with the previous theoretical predictions [1,7,28] and can be explained by Eq. (2) [3,31]. According to Eq. (2), increasing sampling time increases $\langle\beta\rangle$, which decreases the overall 2D peak capacity. However, increasing the sampling time increases the second dimension peak capacity, which increases the overall 2D peak capacity. These two opposing effects result in an optimum sampling time which gives a maximum in the corrected 2D peak capacity. In addition, as indicated by the positions of the arrows in this figure, when the first dimension gradient time is shorter than 12 min, the optimum sampling time is about 12 s. Upon increasing the first dimension gradient time, the optimum sampling time shifts to longer times.

We studied the dependence of the second dimension peak capacity production rate on the second dimension gradient time with different 10-port valve configurations (Fig. S3). The results show that the maximum second dimension peak capacity production rate is always obtained when the sampling time is about 10 s.

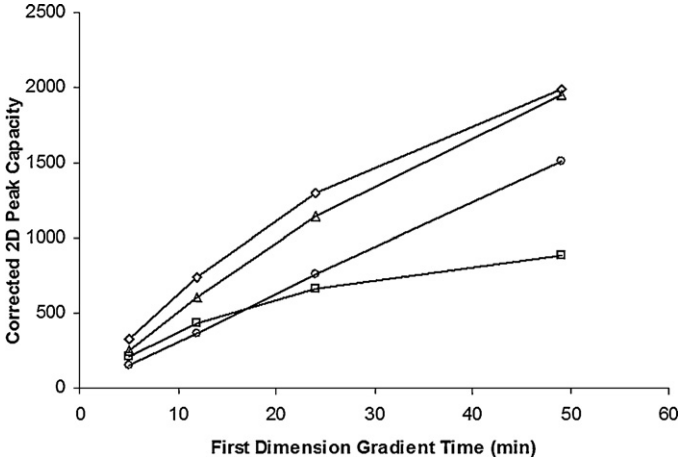

Fig. 3. Corrected 2D peak capacity of on-line two dimensional liquid chromatography as a function of first dimension gradient time. Sampling times are 12 s (◊); 21 s (△); 40 s (○); 6 s (□). All corrected 2D peak capacity was corrected by under-sampling effect using Eqs. (2) and (3), with $f_{coverage}$ set to unity. Values of ${}^1n_c$, ${}^2n_c$ and $\langle\beta\rangle$ for the corrected 2D peak capacity calculation are given in Table 3.

Therefore, when the first dimension gradient time is short, the optimum sampling time (~12 s) is close to the time which maximizes the peak capacity production rate (~10 s). However, upon increasing the first dimension gradient time, the optimum sampling time shifts to longer times and therefore, departs more from the value corresponding to the maximum second dimension peak capacity production rate. This trend is consistent with Eq. (4) [1]. According to this equation, when under-sampling is severe, the maximum corrected 2D peak capacity will be obtained at an optimum sampling time corresponding to the maximum second dimension peak capacity production rate.

According to Table 2, when the first dimension gradient time is increased from 5 to 49 min, the corresponding average first dimension peak width (taken at 4σ) increases. At shorter first dimension gradient times, the first dimension peaks are narrower and the under-sampling effect is more severe. As a result, the optimum sampling time is closer to the sampling time corresponding to the maximum second dimension peak capacity production rate as predicted by Eq. (4). According to Eq. (4), when the under-sampling effect is severe, the corrected 2D peak capacity should increase linearly with the first dimension gradient time. This is clearly observed in Fig. 3. Fig. 3 shows the corrected 2D peak capacities as a function of first dimension gradient times. It is apparent that the dependence of the peak capacity on the first dimension gradient time becomes progressively more linear as the sampling time increases beyond 12 s. This is because upon increasing sampling time, the sampling rate decreases, resulting in more serious under-sampling effects and the linear increase in the corrected 2D peak capacity against the first dimension gradient time predicted by the simplified equation becomes more evident.

4.2. Comparison of experimental 1D and 2D separations

Fig. 2 shows the maximum corrected 2D peak capacity that on-line LC × LC can achieve in 1 h is about 2000. However, such high peak capacity is obtained based on the assumption that the coverage factor, $f_{coverage}$ is unity for on-line LC × LC. Unity $f_{coverage}$ means that the peaks must distribute fully and occupy the entire 2D separation space; this is simply not true for real 2D experiments. According to prior work from this lab [3], a typical $f_{coverage}$ for the maize seed extract sample is between 0.5 and 0.7, which gives an effective peak capacity of only ~50–70% of the 2D peak capacity calculated in Fig. 2. Thus, a fair comparison of 1DLC and on-line

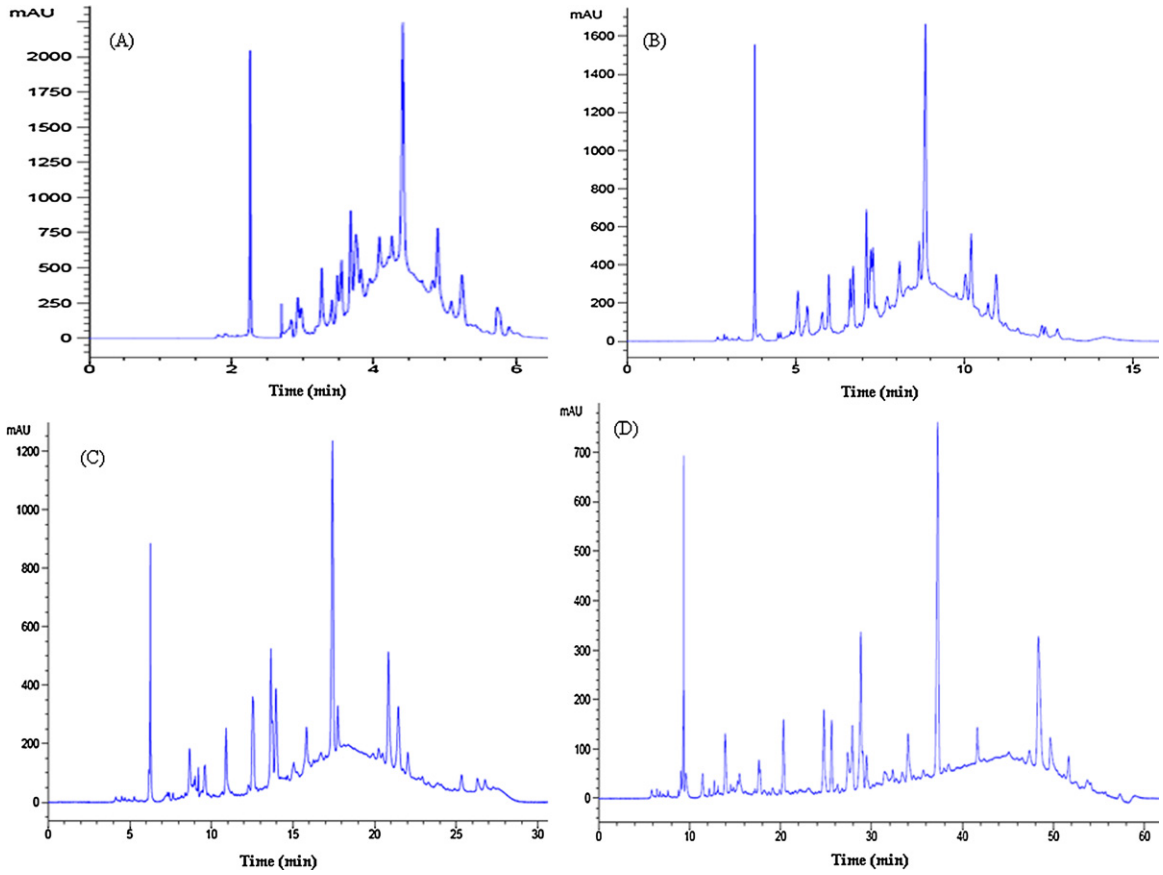

Fig. 4. Chromatograms of maize seed extract separated by fully optimized one dimensional liquid chromatography. (A) Gradient time = 5 min (number of observed peaks = 40, ${}^1n_c = 100$). (B) Gradient time = 12 min (number of observed peaks = 60, ${}^1n_c = 135$). (C) Gradient time = 24 min (number of observed peaks = 88, ${}^1n_c = 150$). (D) Gradient time = 49 min (number of observed peaks = 100, ${}^1n_c = 163$).

LC × LC separation power must consider how the separation space is used in both methodologies. Fig. 4 shows chromatograms for the maize seed extract under the fully optimized 1DLC conditions (see Table 1). All of these chromatograms show that the peaks are distributed over the whole gradient time window. Furthermore, in each gradient time window, peaks seem to be lumped together, without leaving any gaps within the gradient time window. Based on these observations, we conclude that in fully optimized 1DLC, the whole separation space was used, with a $f_{coverage}$ value corresponding to unity.

Some representative examples of the on-line LC × LC separations of the maize seed extract at different first and second dimension gradient times are given in Figs. 5 and 6. These figures clearly show that in on-line LC × LC, the separation space is only partially occupied. To accurately evaluate how the separation space is used in on-line LC × LC, the chromatographic peaks observed in the on-line LC × LC were counted by visual inspection as described above and retention times for the detected peaks were recorded. The distribution of the detected peaks was then used to estimate $f_{coverage}$ according to the procedure described in Section 3.4 and illustrated in Fig. S1. The $f_{coverage}$ values obtained for each first and second dimension gradient time combination are given in Table 3. These $f_{coverage}$ values were used to calculate the effective 2D peak capacities according to Eq. (2). The effective 2D peak capacities, and the peak capacity of the fully optimized 1DLC, were then plotted against gradient time in Fig. 7. In Fig. 7, the abscissa refers to first dimension gradient time and gradient time for on-line LC × LC and 1DLC, respectively. This figure allows us to compare the peak capacities of 1DLC and on-line LC × LC based on the same time used for separations. Comparison of Figs. 3 and 7 shows that in contrast to Fig. 3 where the maximum corrected 2D peak capacities were always obtained when the sampling time was 12 s, the optimum sampling time now varies with the first dimension gradient time. When the first dimension gradient time is less than 24 min, the maximum *effective* 2D peak capacities were obtained when sampling time was 12 s. When the first dimension gradient time was increased to 24 and 49 min, the maximum *effective* 2D peak capacities were obtained when the sampling time was 21 s. This comparison shows that the coverage factor plays an important role in determining the optimum sampling time for the maximum effective 2D peak capacity. That is, the coverage factor varies significantly with the sampling time especially when it is very short. Most importantly, both Figs. 3 and 7 show that the maximum 2D peak capacity is always obtained at an intermediate sample time between 12 and 21 s although there is not much difference between these two times. In addition, according to Fig. 7, the crossover time at which on-line LC × LC and fully optimized 1DLC have comparable resolving power is a function of sampling time. For sampling times of 12 and 21 s, the crossover time is the shortest, about 5 min. It should be noted that at a first dimension gradient time of 5 min, the effective 2D peak capacities at sampling times of 12 and 21 s are slightly higher than the peak capacity of fully optimized 1DLC. When the sampling time is 40 s, the crossover time increases to 7 min. The longest crossover time (about 15 min) is obtained when the sampling time is 6 s. Contrary to intuitive thinking the fastest sampling time does not give the shortest crossover time. This results because one sacrifices too much second dimension peak capacity by going to short sampling times. Finally, upon increasing the first dimension gradient time, bigger improvements in the effective 2D peak capacity relative to fully optimized 1DLC

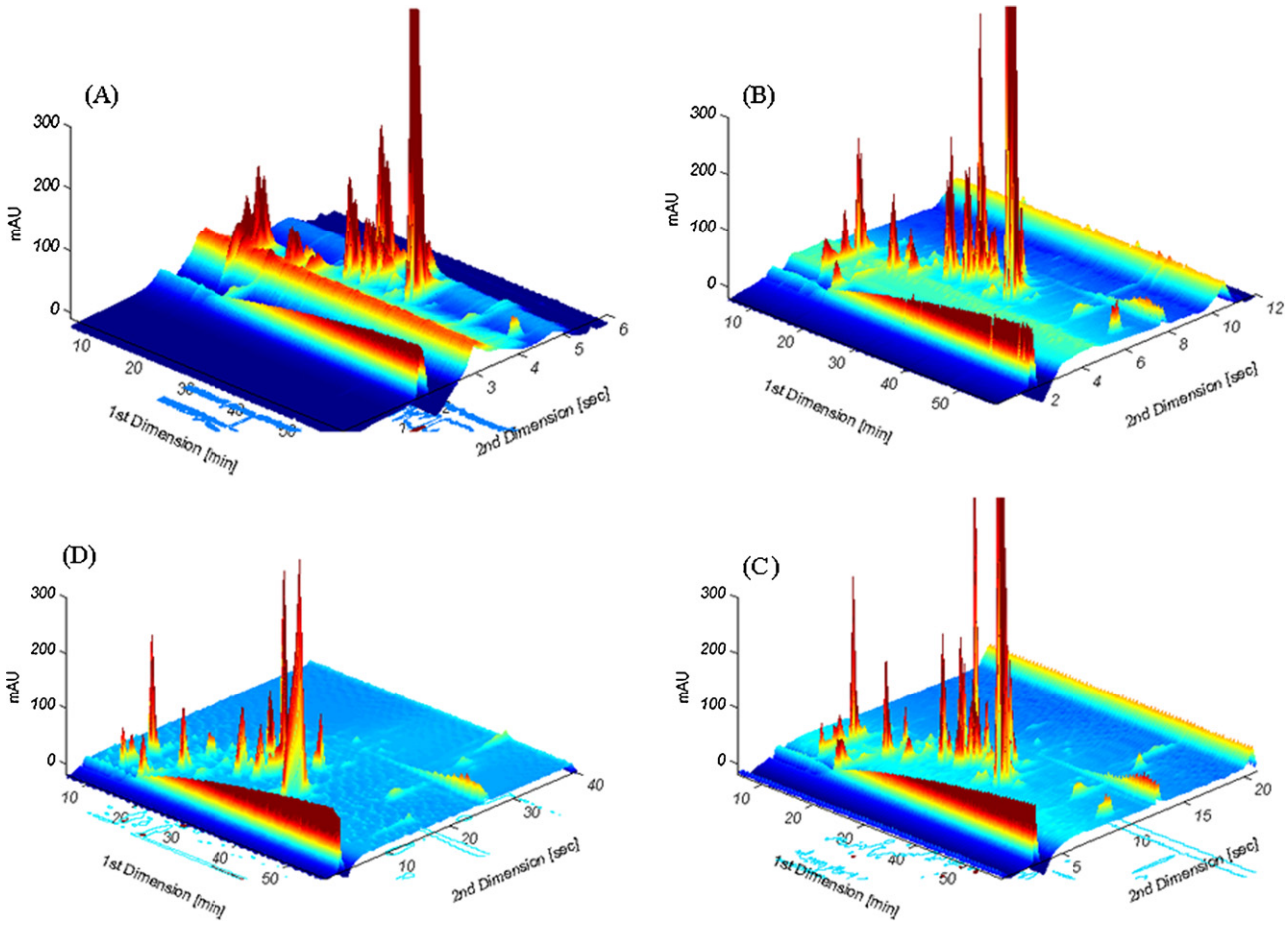

Fig. 5. Effect of sampling time on the two dimensional chromatogram of maize seed extract. First dimension gradient time is 49 min in all cases. (A) t_s = 6 s; (B) t_s = 12 s; (C) t_s = 21 s; (D) t_s = 40 s.

Table 3
Comparison of on-line two dimensional liquid chromatography and fully optimized one dimensional liquid chromatography in terms of peak capacities and the number of observed peaks in maize seed extract separations.

^1t_g (min)[a]	t_s (s)[b]	^1n_c[c]	$\langle\beta\rangle$[d]	^2n_c[e]	$f_{coverage}$[f]	$n_{c,\,2D}{}^*$[g]	P_{1D}[h]	P_{2D}/P_{1D}[i]	$n_{c,\,2D}{}^*/n_{c,1D}$[j]
5	6	27	1.404	11	0.30	63	40	0.32	0.63
	12	27	2.210	27	0.45	149	40	0.80	1.5
	21	27	3.590	34	0.45	116	40	0.80	1.2
	40	27	6.643	38	0.51	79	40	0.75	0.79
12	6	58	1.337	10	0.25	108	60	0.41	0.80
	12	58	2.036	26	0.51	384	60	1.1	2.8
	21	58	3.261	34	0.54	325	60	1.2	2.4
	40	58	5.996	38	0.51	187	60	0.92	1.4
24	6	78	1.162	10	0.35	236	88	0.42	1.6
	12	78	1.550	26	0.58	754	88	1.4	5.0
	21	78	2.301	34	0.67	769	88	1.6	5.1
	40	78	4.072	40	0.56	430	88	1.2	2.9
49	6	94	1.060	10	0.31	276	100	0.60	1.7
	12	94	1.221	26	0.53	1054	100	1.7	6.5
	21	94	1.582	33	0.59	1146	100	1.9	7.1
	40	94	2.540	41	0.48	732	100	1.5	4.5

[a] First dimension gradient time in on-line LC × LC or gradient time in fully optimized 1DLC.
[b] Sampling time. Equal to the second dimension cycle time.
[c] First dimension peak capacity as shown in Table 2.
[d] First dimension peak broadening factor calculated by Eq. (3) using t_s and first dimension average peak width listed in Table 2.
[e] Second dimension peak capacity calculated using the average peak width of maize seed extract separated by on-line LC × LC.
[f] Coverage factor.
[g] Effective 2D peak capacity calculated by Eqs. (2) and (3).
[h] Number of real peaks observed in maize seed extract separated by fully optimized 1DLC.
[i] Ratio of the number of real peaks observed in maize seed extract separated by on-line LC × LC to fully optimized 1DLC.
[j] Ratio of effective 2D peak capacity to fully optimized 1DLC peak capacity.

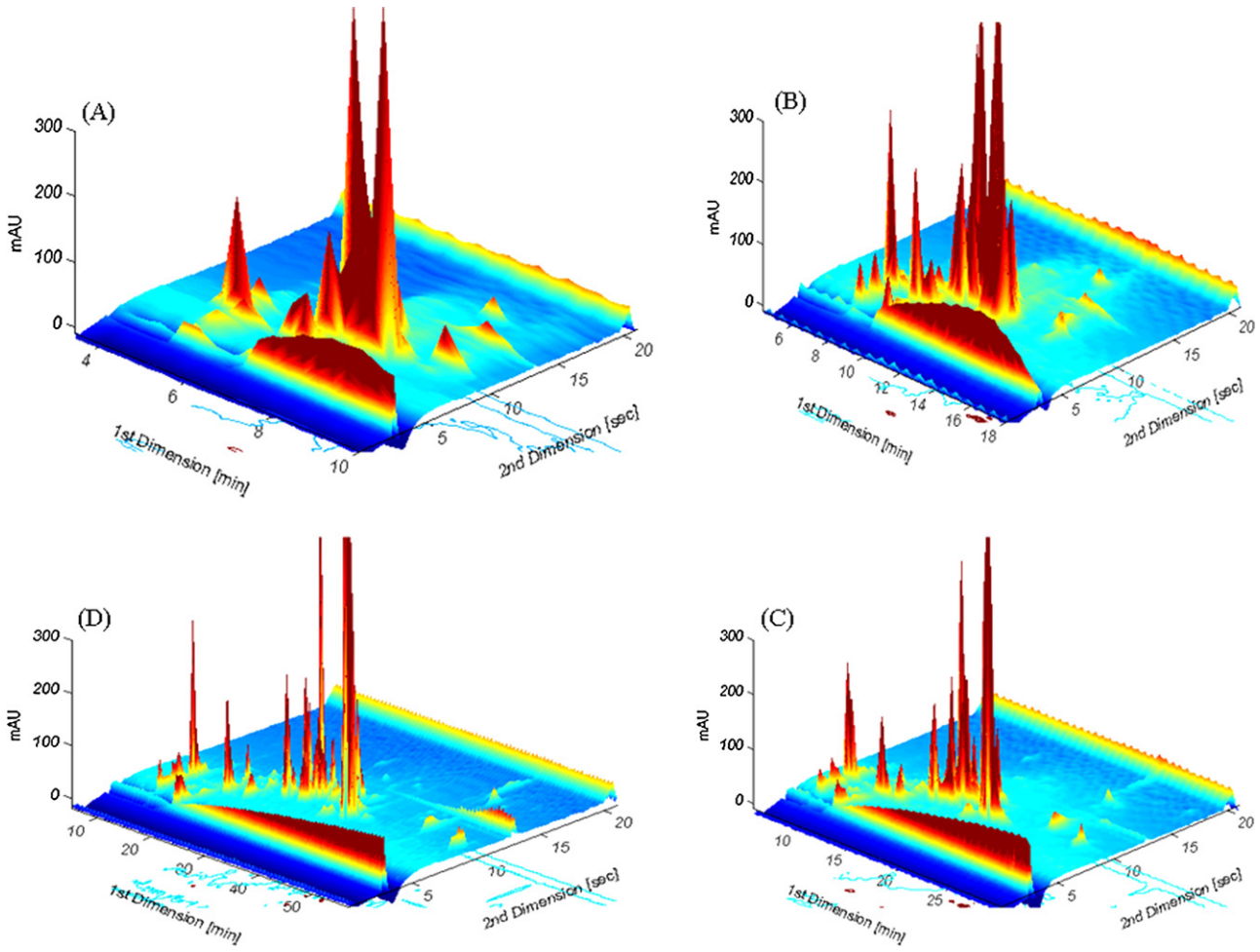

Fig. 6. Effect of first dimension gradient time on the two dimensional chromatogram of maize seed extract. Sampling time is 21 s in all cases. (A) ${}^1t_g$ = 5 min; (B) ${}^1t_g$ = 12 min; (C) ${}^1t_g$ = 24 min; (D) ${}^1t_g$ = 49 min.

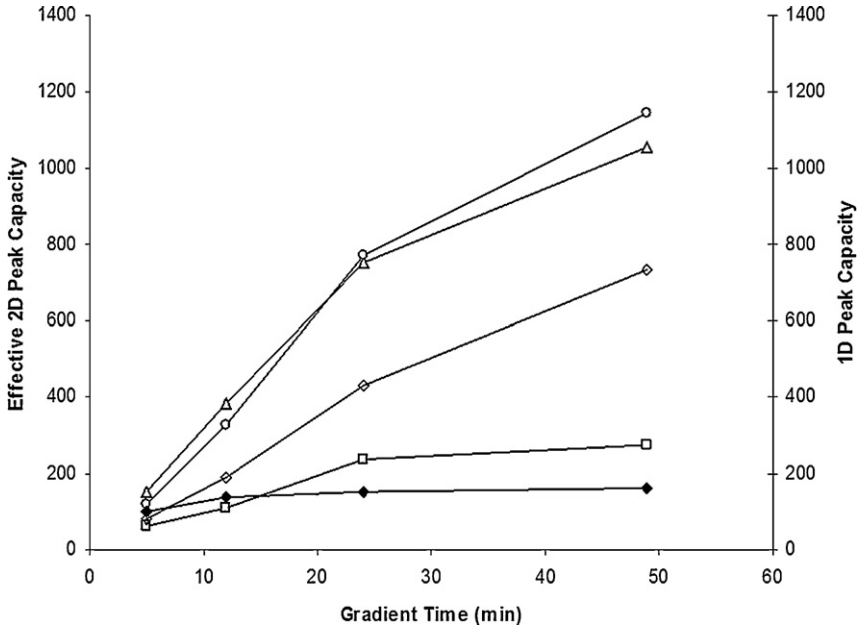

Fig. 7. Comparison of the effective 2D peak capacity of on-line two dimensional liquid chromatography with peak capacity of fully optimized one dimensional liquid chromatography. The effective 2D peak capacity was calculated by Eqs. (2) and (3), considering both the under-sampling and coverage factor effects. Values of ${}^1n_c$, ${}^2n_c$, $\langle\beta\rangle$ and $f_{coverage}$ for effective 2D peak capacity calculation are given in Table 3. Second dimension cycle times are 21 s (○); 12 s (△); 40 s (◊); 6 s (□). Fully optimized one dimensional LC is denoted by (♦).

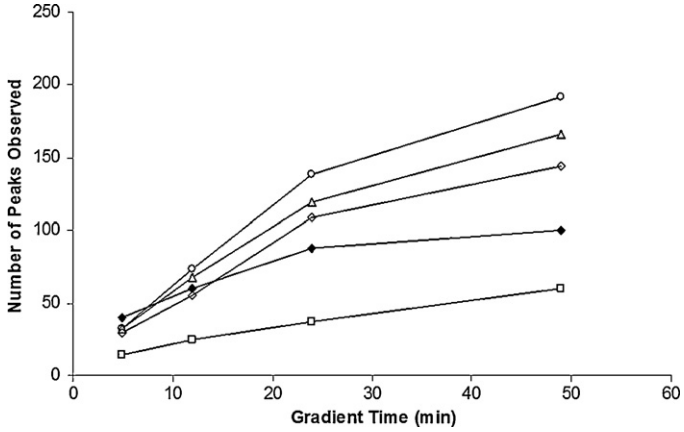

Fig. 8. Comparison of number of peaks observed by on-line two dimensional liquid chromatography and fully optimized one dimensional liquid chromatography in the separation of a maize seed extract sample. Second dimension cycle times are 21 s (○); 12 s (△); 40 s (◊); 6 s (□). Fully optimized one dimensional LC is denoted by (♦).

are obtained. According to Fig. 7, even when we consider both the $f_{coverage}$ and under-sampling effect, improvements of up to 7-fold in peak capacities can be obtained by on-line LC × LC as compared to fully optimized 1DLC.

The number of peaks observed in fully optimized 1DLC and on-line LC × LC are compared in Fig. 8. The abscissa is the gradient time. The ordinate is the number of peaks found by on-line LC × LC and fully optimized 1DLC. The comparison of the number of peaks observed is a very complex issue. Due to the higher resolving power of LC × LC one certainly expects to see more peaks by this technique when a very complex natural sample such as a maize extract is examined. However, the impact of greater dilution of the sample in 2D separations must also be considered. Not only is the sample diluted during each chromatographic step but the gradient baseline is much steeper in the fast second dimension separation making it more difficult to detect peaks. We cannot really compensate for the increased difficulty of peak detection in LC × LC but it is definitely a serious issue. We are convinced that if baseline irregularities could be improved we would see even more peaks by LC × LC.

In order to check the impact of the valve configuration on peak number, the experiment at ${}^1t_g = 24$ min was repeated at the four different sampling time using the FIFO valve configuration. An Agilent 1200 binary pump together with a 35 μL Agilent Jet Weaver mixer was used for the fast gradient elution in the second dimension. In comparison to the results repeated in Fig. 8, we found the change in peak numbers was 16.6%, 11.3%, 5.4% and 1.9% at the four sampling times shown in Fig. 8. Therefore, the differences in peak numbers caused by the different valve configurations are judged to be essentially the same. Fig. 8 shows that upon increasing the first dimension gradient time, the number of observed peaks in LC × LC increases more rapidly than in fully optimized 1DLC. At a sufficiently long first dimension gradient time even the numbers of observed peaks with a sampling time of 6 s will exceed the peak numbers of 1DLC.

Such a trend is similar to that observed in Fig. 7, in which the resolving power is evaluated in terms of the effective 2D peak capacity. At the longest first dimension gradient time studied here (49 min), the number of maize seed extract peaks observed by on-line LC × LC separation can be up to almost twice the number of peaks found by fully optimized 1DLC. Comparison of Fig. 7 to Fig. 8 shows a similar trend in crossover time based on the number of observed peaks and the effective peak capacity. For sampling times of 12 and 21 s, the crossover time is the shortest (about 7 min). At a gradient time of 5 min, the numbers of observed peaks for all four sampling times are lower than that of the fully optimized 1DLC. When the sampling time is 40 s, the crossover time increases (15 min). The longest crossover time is obtained when the sampling time is 6 s. Therefore, based on use of both the effective peak capacity and the numbers of observed peaks as metrics of the resolving power, the crossover time for 1DLC and on-line LC × LC is about 5–7 min when the correct sampling time (12–21 s) is used. These results are consistent with both previously published experimental work [3,39] and recent calculations.

It should be pointed out that the resolving power comparison here was carried out on the instrument systems currently available in our lab. If we were to operate the fully optimized 1DLC using a UPLC system, higher 1DLC peak capacities would be obtained. However, computer calculations based on a standard mixture of twelve indole acetic acid derivatives indicate that at a column temperature of 40 °C, when particle size is fixed at 5 μm and gradient time is fixed at 60 min, under the conditions that column length, flow rate and gradient mobile phase compositions are fully optimized, there would be only 28% gain in peak capacity by increasing the maximum system pressure from 400 to 1200 bar. Therefore, using UPLC for the fully optimized 1DLC separation would not change our major conclusions as to the relative resolving power of 1DLC and on-line LC × LC. In addition, if we were to increase the maximum system pressure in the second dimension and therefore, increase the second dimension peak capacity at a given sampling time, we would be able to increase the overall resolving power of on-line LC × LC. However, due to pressure limitations imposed by both the second dimension pump and the 10-port valve, we had to restrict the maximum pressure used in the second dimension to 400 bar.

5. Conclusions

In this work, the effects of sampling time on the resolving power of on-line LC × LC were studied and compared to that of 1DLC in terms of both their effective peak capacities and the number of chromatographic peaks observed based in separation of a maize seed extract. The principal conclusions are as follows:

Sampling time has a very large impact on the resolving power of on-line LC × LC. Based on both metrics (peak capacity and number of observed peaks) the maximum resolving power is always obtained at an intermediate sampling time of 12–21 s. This result is consistent with previous theoretical studies [1,7,28].

Based on both metrics, we conclude that the crossover time for fully optimized 1DLC and on-line LC×LC working in the optimum sampling time range (12–21 s) is 5–7 min; this is consistent with previously reported experiments [3] and more recent calculations [39]. Shorter and longer sampling times outside the optimum range lead to longer crossover times.

The resolving power of on-line LC × LC can be significantly improved by increasing the first dimension gradient time. At the longest first dimension gradient time studied here (49 min), up to a 7-fold increase in the *effective* 2D peak capacity and almost a 2-fold improvement in the number of observed peaks was obtained in on-line LC × LC relative to1DLC.

The coverage factor is very important to the value of the effective 2D peak capacity. It decreases at very short sampling times.

Acknowledgement

This work was supported by a grant from NIH (GM 054585). We also wish to acknowledge funding from the Agilent Foundation and the gifts of columns from Supelco Inc. and ZirChrom Separations Inc. The authors wish to thank Dr. Wenzhe Fan and especially Prof. Dwight Stoll for many helpful conversations during the course of this work. The authors also wish to thank Klaus Witt of Agilent Technologies for his many valuable suggestions.

Appendix A. Supplementary data

Supplementary data associated with this article can be found, in the online version, at doi:10.1016/j.chroma.2011.03.032.

References

[1] X. Li, D.R. Stoll, P.W. Carr, Anal. Chem. 81 (2009) 845.
[2] G.J. Opiteck, J.W. Jorgenson, R.J. Anderegg, Anal. Chem. 69 (1997) 2283.
[3] D.R. Stoll, X. Wang, P.W. Carr, Anal. Chem. 80 (2008) 268.
[4] D.R. Stoll, J.D. Cohen, P.W. Carr, J. Chromatogr. A 1122 (2006) 123.
[5] D.R. Stoll, X. Li, X. Wang, S.E.G. Porter, S.C. Rutan, P.W. Carr, J. Chromatogr. A 1168 (2007) 3.
[6] D.R. Stoll, P.W. Carr, J. Am. Chem. Soc. 127 (2005) 5034.
[7] K. Horvath, J.N. Fairchild, G. Guiochon, Anal. Chem. 81 (2009) 3879.
[8] K. Horvath, J. Fairchild, G. Guiochon, J. Chromatogr. A 1216 (2009) 2511.
[9] F. Bedani, W.T. Kok, H.G. Janssen, Anal. Chim. Acta 654 (2009) 77.
[10] F. Bedani, H.G. Janssen, LC–GC Eur. 22 (2009) 248.
[11] H.J. Issaq, K.C. Chan, G.M. Janini, T.P. Conrads, T.D. Veenstra, J. Chromatogr. B 817 (2005) 35.
[12] W.B. Dunn, D.I. Ellis, Trac—Trend. Anal. Chem. 24 (2005) 285.
[13] G. Guiochon, J. Chromatogr. A 1126 (2006) 6.
[14] I. François, K. Sandra, P. Sandra, Anal. Chim. Acta 641 (2009) 14.
[15] P. Schoenmakers, P. Marriott, J. Beens, LC–GC Eur. 16 (2003) 335.
[16] C.X. Song, M.L. Ye, G.H. Han, X.N. Jiang, F.J. Wang, Z.Y. Yu, R. Chen, H.F. Zou, Anal. Chem. 82 (2010) 53.
[17] L. Mondello, P. Donato, F. Cacciola, C. Fanali, P. Dugo, J. Sep. Sci. 33 (2010) 1454.
[18] I. Francois, D. Cabooter, K. Sandra, F. Lynen, G. Desmet, P. Sandra, J. Sep. Sci. 32 (2009) 1137.
[19] M. Kivilompolo, V. Oburka, T. Hyotylainen, Anal. Bioanal. Chem. 391 (2008) 373.
[20] P. Dugo, F. Cacciola, P. Donato, D. Airado-Rodriguez, M. Herrero, L. Mondello, J. Chromatogr. A 1216 (2009) 7483.
[21] J. Adrian, E. Esser, G. Hellmann, H. Pasch, Polymer 41 (2000) 2439.
[22] H. Pasch, M. Adler, F. Rittig, S. Becker, Macromol. Rapid. Commun. 26 (2005) 438.
[23] J.A. Raust, A. Brull, C. Moire, C. Farcet, H. Pasch, J. Chromatogr. A 1203 (2008) 207.
[24] H.G. Janssen, H. Steenbergen, S. de Koning, Eur. J. Lipid. Sci. Technol. 111 (2009) 1171.
[25] J.N. Fairchild, K. Horvath, G. Guiochon, J. Chromatogr. A 1216 (2009) 6210.
[26] J.N. Fairchild, K. Horvath, G. Guiochon, J. Chromatogr. A 1216 (2009) 1363.
[27] G. Guiochon, N. Marchetti, K. Mriziq, R.A. Shalliker, J. Chromatogr. A 1189 (2008) 109.
[28] K. Horie, H. Kimura, T. Ikegami, A. Iwatsuka, N. Saad, O. Fiehn, N. Tanaka, Anal. Chem. 79 (2007) 3764.
[29] R.E. Murphy, M.R. Schure, J.P. Foley, Anal. Chem. 70 (1998) 1585.
[30] J.V. Seeley, J. Chromatogr. A 962 (2002) 21.
[31] J.M. Davis, D.R. Stoll, P.W. Carr, Anal. Chem. 80 (2008) 461.
[32] M. Gilar, A.E. Daly, M. Kele, U.D. Neue, J.C. Gebler, J. Chromatogr. A 1061 (2004) 183.
[33] L.W. Potts, X. Li, D.R. Stoll, P.W. Carr, J. Chromatogr. A 1217 (2010) 5700.
[34] X. Wang, W.E. Barber, P.W. Carr, J. Chromatogr. A 1107 (2006) 139.
[35] X. Wang, D.R. Stoll, P.W. Carr, P.J. Schoenmakers, J. Chromatogr. A 1125 (2006) 177.
[36] X. Wang, D.R. Stoll, A.P. Schellinger, P.W. Carr, Anal. Chem. 78 (2006) 3406.
[37] G. Vivo-Truyols, S. van der Wal, P.J. Schoenmakers, Anal. Chem. 82 (2010) 8525.
[38] P.J. Schoenmakers, G. Vivo-Truyols, W.M.C. Decrop, J. Chromatogr. A 1120 (2006) 282.
[39] H. Gu, Y. Huang, P.W. Carr, J. Chromatogr. A 1218 (2011) 64.
[40] L.R. Snyder, J.L. Glajch, J.J. Kirkland, Practical HPLC Method Development, Wiley & Sons, New York, 1996.
[41] J.D. Thompson, J.S. Brown, P.W. Carr, Anal. Chem. 73 (2001) 3340.
[42] A.P. Schellinger, D.R. Stoll, P.W. Carr, J. Chromatogr. A 1192 (2008) 43.
[43] A.P. Schellinger, D.R. Stoll, P.W. Carr, J. Chromatogr. A 1192 (2008) 54.
[44] S. Peters, G. Vivo-Truyols, P.J. Marriott, P.J. Schoenmakers, J. Chromatogr. A 1156 (2007) 14.